Published online 13 January 2020 *Nucleic Acids Research, 2020, Vol. 48, No. 4* **2013–2025**
doi: 10.1093/nar/gkz1200

Dynamics of DNA nicking and unwinding by the RepC–PcrA complex

Carolina Carrasco[1,*], Cesar L. Pastrana[1], Clara Aicart-Ramos[1], Sanford H. Leuba[2], Saleem A. Khan[3] and Fernando Moreno-Herrero[1,*]

[1]Department of Macromolecular Structures, Centro Nacional de Biotecnología, CSIC, Darwin 3, 28049 Cantoblanco, Madrid, Spain, [2]Departments of Cell Biology and Bioengineering, UPMC Hillman Cancer Center, University of Pittsburgh School of Medicine, 5117 Centre Avenue, Pittsburgh, PA 15213, USA and [3]Department of Microbiology and Molecular Genetics, University of Pittsburgh School of Medicine, 450 Technology Drive, Pittsburgh, PA 15219, USA

Received June 06, 2019; Revised December 10, 2019; Editorial Decision December 12, 2019; Accepted December 18, 2019

ABSTRACT

The rolling-circle replication is the most common mechanism for the replication of small plasmids carrying antibiotic resistance genes in Gram-positive bacteria. It is initiated by the binding and nicking of double-stranded origin of replication by a replication initiator protein (Rep). Duplex unwinding is then performed by the PcrA helicase, whose processivity is critically promoted by its interaction with Rep. How Rep and PcrA proteins interact to nick and unwind the duplex is not fully understood. Here, we have used magnetic tweezers to monitor PcrA helicase unwinding and its relationship with the nicking activity of *Staphylococcus aureus* plasmid pT181 initiator RepC. Our results indicate that PcrA is a highly processive helicase prone to stochastic pausing, resulting in average translocation rates of 30 bp s^{-1}, while a typical velocity of 50 bp s^{-1} is found in the absence of pausing. Single-strand DNA binding protein did not affect PcrA translocation velocity but slightly increased its processivity. Analysis of the degree of DNA supercoiling required for RepC nicking, and the time between RepC nicking and DNA unwinding, suggests that RepC and PcrA form a protein complex on the DNA binding site before nicking. A comprehensive model that rationalizes these findings is presented.

INTRODUCTION

Plasmids are circular double-stranded DNA molecules present in bacterial cells that are replicated independently of the chromosome (1). Transmission of plasmids between cells results in gain of function to the recipient cell; thus, the interest in plasmid biology ranges from basic research to applied biotechnology. At the fundamental level, plasmids can be transferred across species, and the acquired genes are spread and subjected to a coevolutionary process. At the applied level, plasmid genes naturally encode resistance to antibiotics (2,3) and to heavy metals (4), and promote the formation of tumours in plants (5). Understanding the mechanisms of dissemination and replication of plasmids is of great relevance for human health, bioremediation, biotechnology and agriculture.

Replication of small (<10 kb), promiscuous, multicopy plasmids carrying antibiotic resistance genes in Gram-positive bacteria generally occurs by the rolling-circle replication (RCR) mechanism (2,3) (Figure 1). The most distinct characteristic of RCR is its initiation step by a replication initiator protein (Rep) encoded by the plasmid. Rep proteins bind specifically to the double-strand origin of replication (*dso*) as a dimer (Figure 1A), and nick one of the DNA strands by a topoisomerase I-like mechanism. This results in the protein becoming covalently bound to the strand to be displaced (*displaced strand*) through a 5′-phosphotyrosine adduct and the formation of a free 3′-OH end at the nick (Figure 1B) (6). The unwinding of the plasmid during RCR is then carried out by a host-encoded superfamily I helicase. In Gram-positive bacteria, this function relies on the nonreplicative helicase PcrA. Rep proteins recruit the PcrA helicase at the nicking site, where the helicase interacts with a short ssDNA fragment (7). The Rep–PcrA complex unwinds the DNA duplex leading to the formation of an ssDNA loop, and DNA polymerase III synthesizes a new strand (*leading strand*) starting from the 3′-OH produced at the nicking site (8) (Figure 1C). The asymmetric nature of this process leads to the formation of ssDNA loops during the helicase unwinding, and

*To whom correspondence should be addressed. Tel: +34 91 585 5305; Email: fernando.moreno@cnb.csic.es
Correspondence may also be addressed to Carolina Carrasco. Email: carolina.carrasco@cnb.csic.es

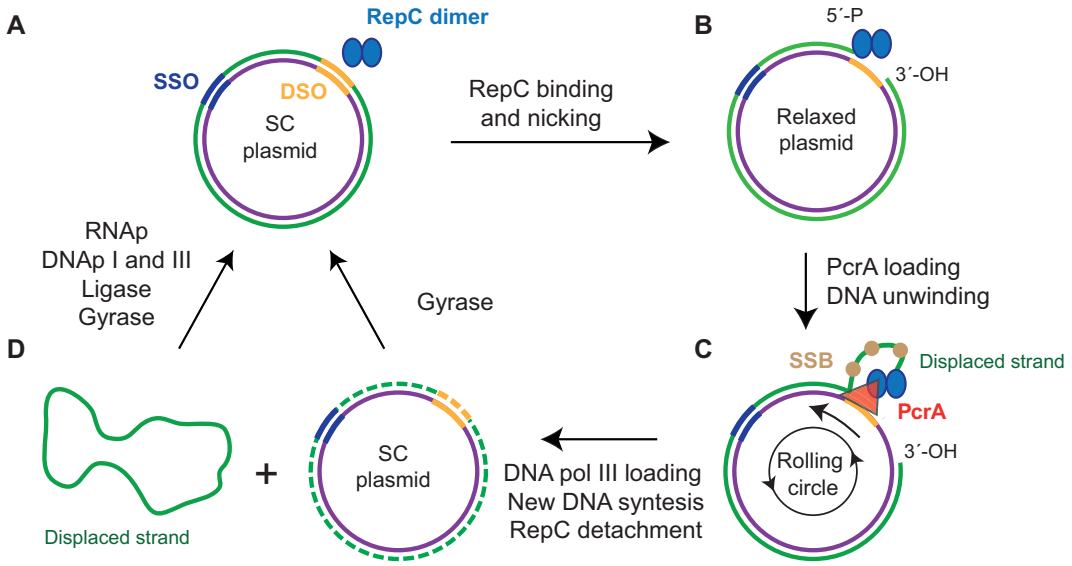

Figure 1. Model of plasmid RCR. (**A**) A supercoiled plasmid containing the origin of replication (*dso*). (**B**) A RepC protein dimer binds to the *dso* and nicks the duplex, remaining covalently attached to the 5′-P end. (**C**) PcrA helicase unwinds the plasmid in complex with RepC producing ssDNA that is further protected from degradation by the SSB protein. The 3′-OH end serves as primer for DNA synthesis by DNA polymerase III. (**D**) In the termination step, the nick is sealed by RepC leading to a relaxed closed circular dsDNA and RepC is detached from the DNA.

single-stranded DNA binding (SSB) proteins interact with the nascent ssDNA to protect it from degradation (9). In the current model, DNA synthesis continues until the *dso* sequence is reached. Then, in a process that is not fully understood, a set of transesterification reactions between the Rep dimer and the DNA combined with the activity of ligases and gyrases produce a replicated dsDNA plasmid and a circular ssDNA originated from the *displaced strand* (Figure 1D). The circular ssDNA is further converted to dsDNA by using the single-strand origin of replication (*sso*) in a process that involves RNA polymerase for RNA primer synthesis and DNA polymerases I and III for replication (10,11).

A key component of the RCR mechanism is the helicase. Although PcrA has been shown to be essential in different Gram-positive organisms, the precise cellular roles of PcrA are not fully understood (12–14). Most of the current knowledge of PcrA biochemistry is based on the *Bacillus stearothermophilus* PcrA (*Bs*PcrA) and the *Staphylococcus aureus* PcrA (*Sa*PcrA). Structural, kinetic and single-molecule analysis of *Bs*PcrA revealed that it is a monomeric protein that unwinds the DNA with 3′–5′ polarity using an inchworm mechanism (15–18). Isolated *Bs*PcrA and *Sa*PcrA have been shown to present very low processivity, the interaction with Rep proteins being necessary for unwinding long duplex DNA substrates (8,16,18–19). This suggests an adaptation of PcrA to function in complex with initiator proteins and a specialization for RCR mechanism. Nevertheless, the precise mechanisms of interaction between Rep proteins and PcrA as well as the dynamics of recruitment of the PcrA helicase to the *dso* remain unsolved. For instance, it is unknown how PcrA loading by Rep might affect the binding and nicking activities of Rep at the *dso* or if PcrA and Rep might form a complex prior to Rep nicking.

The pT181 tetracycline resistance plasmid of *S. aureus* has been considered a model system for RCR studies (2,3). It encodes the 38-kDa homodimeric replication initiation protein RepC that has been extensively characterized at the biochemical level (20–23). In a previous report, we found that while nicking by RepC only occurs at negative twist of the DNA, RepC can bind to relaxed DNA molecules. Nicking was also found to be dependent on DNA stretching force and twisting. We concluded that the combination of force and twist was critical for the formation of the DNA secondary structure, namely the extrusion of a cruciform structure at the *dso*, required for RepC nicking (24). A recent report using RepD, the replication initiation protein of plasmid pC221, confirmed the requirement of negative twist on the DNA for RepD nicking (25).

Following our previous work, we have now included the *Sa*PcrA helicase in the RCR reaction and investigated the dynamics of PcrA unwinding and RepC nicking using magnetic tweezers (MT). We report highly processive DNA unwinding activities with variable velocities and the presence of stochastic short pauses. The velocity was not affected by helicase concentration, supporting that our measurements report single-molecule events. The presence of SSB protein to prevent the formation of secondary structures in nascent ssDNA slightly increased the processivity of PcrA but did not affect the average velocity or the frequency of pausing of the helicase. Our data show that PcrA unwinding requires previous nicking by RepC and that both proteins can form a complex on the DNA before nicking. This complex alters the degree of DNA supercoiling needed for RepC nicking. We propose that this change of supercoiling degree arises from a conformational change in RepC that affects the relative position of the DNA within the catalytic site of RepC in the RepC–PcrA complex.

MATERIALS AND METHODS

Proteins

MBP-fused wild-type RepC and mutant RepC^{Y191S} proteins were purified as described in (26) with some modifications detailed in Supplementary Methods and Supplementary Figure S1A.

The His–PcrA fusion protein, in which a His6 epitope is fused to the N-terminal end of PcrA, was cloned and purified as described earlier (8).

Escherichia coli SSB protein was kindly provided by Prof. Mark S. Dillingham (University of Bristol).

DNA substrates

The pBlueScriptIISK:pT181*cop608* (7217 bp) plasmid was generated by ligating the pBlueScriptIISK+ plasmid (Stratagene) and the pT181*cop608* plasmid (4257 bp) at their KpnI sites (27).

DNA constructs for MTs consisted of a central fragment produced from the pBlueScriptIISK:pT181*cop608* plasmid ligated to two digoxigenin- or biotin-labelled DNA handles (24,27). A DNA substrate, named the *long-run* DNA, was constructed by digesting the plasmid with BmtI and NcoI enzymes (both from NEB). This resulted in a final product of 7104 bp with the *dso* region located at 5254 bp from the biotinylated (bead) handle. Another DNA construct, named the *short-run* DNA, containing the *dso* at 1623 bp from the biotinylated end was also produced by digesting the pBlueScriptIISK:pT181*cop608* plasmid with BamHI and NotI enzymes. This resulted in a final product of 7198 bp. Handles were PCR generated from the plasmid pSP73-JY0 (28) or pBlueScriptSK+ (Stratagene) using appropriate oligos (Supplementary Table S1) incorporating Dig-dUTP or Bio-dUTP (Roche) in the reaction followed by restriction with BmtI and NcoI (for the *long-run* DNA) or with NotI and BamHI enzymes (for the *short-run* DNA). Subsequent ligation (T4 DNA ligase, NEB) of the handles with the central fragment resulted in the final DNA substrate ready for use in MT experiments. This procedure allowed us to obtain a high yield of torsionally constrained (tc) DNA molecules for MT experiments. We avoided the exposure of the DNA to intercalating agents as well as to UV light during the production of all DNA substrates.

MT assays

We used the MT set-up described by Pastrana et al. (24) similar to the system reported previously (29,30). Description of the technique and details regarding resolution of our MT instrument can be found in (24). Raw data were recorded at 60 Hz and filtered to 3 Hz for representation and analysis. Force values were calculated using the Brownian motion method applied to a DNA-tethered bead (30) and corrected for low-pass filtering and aliasing (31,32). All our experiments were performed at a 0.4 pN stretching force. To minimize nonspecific attachments of proteins and beads, the liquid chamber was pre-incubated with 0.1 mg ml^{-1} bovine serum albumin (BSA).

Single-molecule nicking experiments were conducted at ambient temperature in a buffer containing 10 mM Tris–HCl, pH 8.0, 100 mM KCl, 10 mM $MgCl_2$, 10% ethylene glycol, and 0.1 mg ml^{-1} BSA and 200 nM RepC monomer. The reaction buffer for nicking–unwinding experiments was supplemented with 8 mM DTT, 5 mM ATP, and PcrA at indicated concentrations. When indicated, 2 μM of *E. coli* SSB proteins were incorporated in the reaction. We used this saturating condition of SSB to ensure a negligible variation of the concentration of free SSB during helicase unwinding. We used *E. coli* SSB to reduce the presence of secondary structures in generated ssDNA.

The standard nicking–unwinding experiment was performed as follows. DNA molecules were first characterized in the working buffer in the absence of proteins by performing rotation curves at low and high forces. This allowed us to select single torsionally constrained tethers and to determine the magnet turns offset with respect to the equilibrium twist of the DNA (R_{max}), obtained at its maximum extension. This value was determined by fitting the extension–rotation curve to a parabolic function $z\,(R) = c + b \cdot R + a \cdot R^2$. R_{max} was determined by taking the derivative of the function and equalling to zero, $R_{max} = -b/2\,a$. The proteins were then incubated with the DNA at positive rotations for ∼2–3 min. RepC nicking and PcrA unwinding activities were triggered by turning the magnets from positive to negative rotations. The difference between the number of magnet turns at the nicking and R_{max} defines the linking number ΔLk or supercoiling degree required for nicking. Enzymes were injected into the fluid chamber at 18 μl min^{-1}.

Conversion from nanometres to unwound base pairs

The number of unwound base pairs was determined from changes in DNA extension considering the different stretching properties of ssDNA and dsDNA. The elastic response of dsDNA to force can be well approximated by the worm-like chain (WLC) model. However, the elastic response of ssDNA is not well described by typical polymer models due to its complex and highly ion-dependent mechanical properties (33). To overcome this limitation, we experimentally determined the mechanical properties of ssDNA from force–extension curves. We produced ssDNA molecules by heating a dilution of the stock of the *long-run* DNA sample in 10 mM Tris (pH 8.0) and 50 mM DTT for 5 min (95°C), followed by fast cooling to 4°C, by placing the sample in ice. This method prevented rehybridization of separated strands as we have previously shown in atomic force microscopy (AFM) experiments (34). We measured the stretching response of ssDNA molecules by varying the force from 0.02 to 35 pN, in the presence and absence of SSB proteins. This procedure allowed us to obtain changes in extension due to DNA unwinding by PcrA under two SSB conditions, 0 and 2 μM (Supplementary Figure S2, Supplementary Methods).

Dwell time analysis

PcrA translocation traces were analysed following an approach similar to that described earlier (35) and adapted to our experimental conditions. In brief, we measured the time required for unwinding 375 bp, a distance that accounts

for three standard deviations of extension fluctuations at 0.4 pN. Velocities were calculated for multiple PcrA translocation traces at different PcrA concentrations in the absence (Supplementary Figure S3A) and presence of SSB protein (Supplementary Figure S3B). Error bars in mean velocity represent the 95% confidence intervals obtained from bootstrapping the data 10 000 times following the description given in (36). A detailed description of the method can be found in Supplementary Methods.

RESULTS

DNA unwinding by single PcrA enzyme

We have previously reported that RepC, the replication initiation protein of the plasmid pT181, only nicks negatively supercoiled DNA containing the *dso* and this activity is force and twist dependent (24). In this study, we aimed to monitor the subsequent step of the RCR process consisting of the unwinding of the DNA duplex by the PcrA helicase.

We used the MT technique to manipulate single DNA molecules by controlling their supercoiling degree at a defined force of 0.4 pN. We generated two tcDNA substrates with appropriate handles to couple one end of the DNA to a magnetic bead and the other end to the glass surface of the fluid chamber (see 'Materials and Methods' section, Figure 2A, and Supplementary Figure S4A). The first DNA substrate was designed with the *dso* located at ∼5.3 kb from the bead position and oriented in a manner that a helicase with 3′–5′ polarity should move towards the bead (*long-run* DNA substrate). TcDNA molecules were first positively supercoiled and incubated with RepC protein in the working buffer (Figure 2B). As expected, we did not observe any nicking event at positive supercoils. In contrast, a sudden increase of extension due to RepC nicking was recorded when DNA was negatively supercoiled as we previously reported (Figure 2C) (24). A similar result has been reported for RepD, the replication initiation protein of the pC221 plasmid (25). Continuous rotation of the magnet in the negative direction (clockwise) allowed us to monitor religation events, as twisting of religated DNA results in a reduction of extension at the low applied force employed in this study (0.4 pN). However, religation events were rare (24) and DNA remained nicked for hundreds of seconds. Importantly, a RepC-nicked DNA molecule necessarily implies that the protein remains covalently attached to the 5′-end at the nicking site via a phosphotyrosine linkage (6).

Next, we injected PcrA together with ATP into the fluid chamber and observed a continuous decrease of DNA extension, i.e. the movement of the bead towards the surface as a result of PcrA helicase activity (Figure 2D). In the example shown here with the *long-run* DNA substrate (Figure 2A), we observed a decrease of extension of ∼1000 nm, corresponding to 4405 bp after conversion of extension into translocated base pairs (see 'Materials and Methods' section and Supplementary Methods). A similar experiment using the *short-run* DNA (see 'Materials and Methods' section and Supplementary Figure S4A) showed a reduction of the extension of the tethered DNA of ∼300 nm, or 1320 bp (Supplementary Figure S4B and C). These data were consistent with the view of PcrA translocating from the *dso* towards the biotinylated DNA end. Current models consider that DNA unwinding is done by PcrA in complex with RepC, dragging the 5′-P end of the nicked strand, which remains covalently bound to the replication initiation protein (26). Since PcrA moves along ssDNA (9), we concluded that PcrA binds to the unnicked strand and translocates towards the bead with 3′–5′ polarity. This necessarily should result in the formation of a growing single-strand loop in the nicked strand and in the production of a nascent ssDNA behind the helicase (Figure 2D). PcrA translocation was not affected by the continuous rotation of the magnets and left the DNA unconstrained (nicked) (Supplementary Figure S5). Again, this is consistent with RepC–PcrA complex moving away from the free 3′-OH required for religation later in the RCR mechanism.

The observed decrease of extension was caused by the production of ssDNA due to PcrA-dependent dsDNA unwinding. At the force employed here (0.4 pN), ssDNA folds into secondary structures effectively having a shorter extension (0.234 nm bp^{-1}) than dsDNA (37). An illustrative example of a nicking–unwinding experiment by RepC and PcrA is included in Supplementary Movie S1. To unambiguously confirm the duplex unwinding activity of PcrA, we performed another experiment where the force was increased up to 10 pN, immediately after nicking was observed (Supplementary Figure S6A). At this force, the extension of ssDNA is larger than the extension of dsDNA (see Supplementary Methods and Supplementary Figure S6B); therefore, unwinding of the duplex would necessarily imply an increase of the extension of the tether. Indeed, we recorded a continuous increase of extension at a velocity similar to those observed at low force (see later) (Supplementary Figure S6C). This experiment also rules out a model where PcrA sits on the *dso* with RepC and reels DNA ahead of it, as it would always imply a reduction of the extension, regardless of the applied force. In ∼14% of activity traces, we observed a sudden recovery of the extension of the tether that we interpreted as a rehybridization event due to detachment of PcrA from the unnicked ssDNA (Supplementary Figure S7A). In ∼5% of all activity traces, additional unwinding was observed again immediately after rehybridization of dsDNA (Supplementary Figure S7B). We did not observe unwinding events in torsionally unconstrained (nicked) DNA (Supplementary Figure S8A), or in supercoiled DNA that was not previously nicked by RepC (Supplementary Figure S8B). These results support the conclusion that PcrA translocation strictly requires a previous nick made by RepC. Other control experiments performed in the absence of ATP, the helicase or the *dso* sequence did not produce any reduction in the extension of the tether that could be attributed to the helicase activity (data not shown). Taken together, we conclude that RepC binding and nicking activities on DNA are required for DNA unwinding by the PcrA helicase.

PcrA unwinding rates and processivity

Next, we characterized the processivity and unwinding velocity of PcrA at different helicase concentrations and the

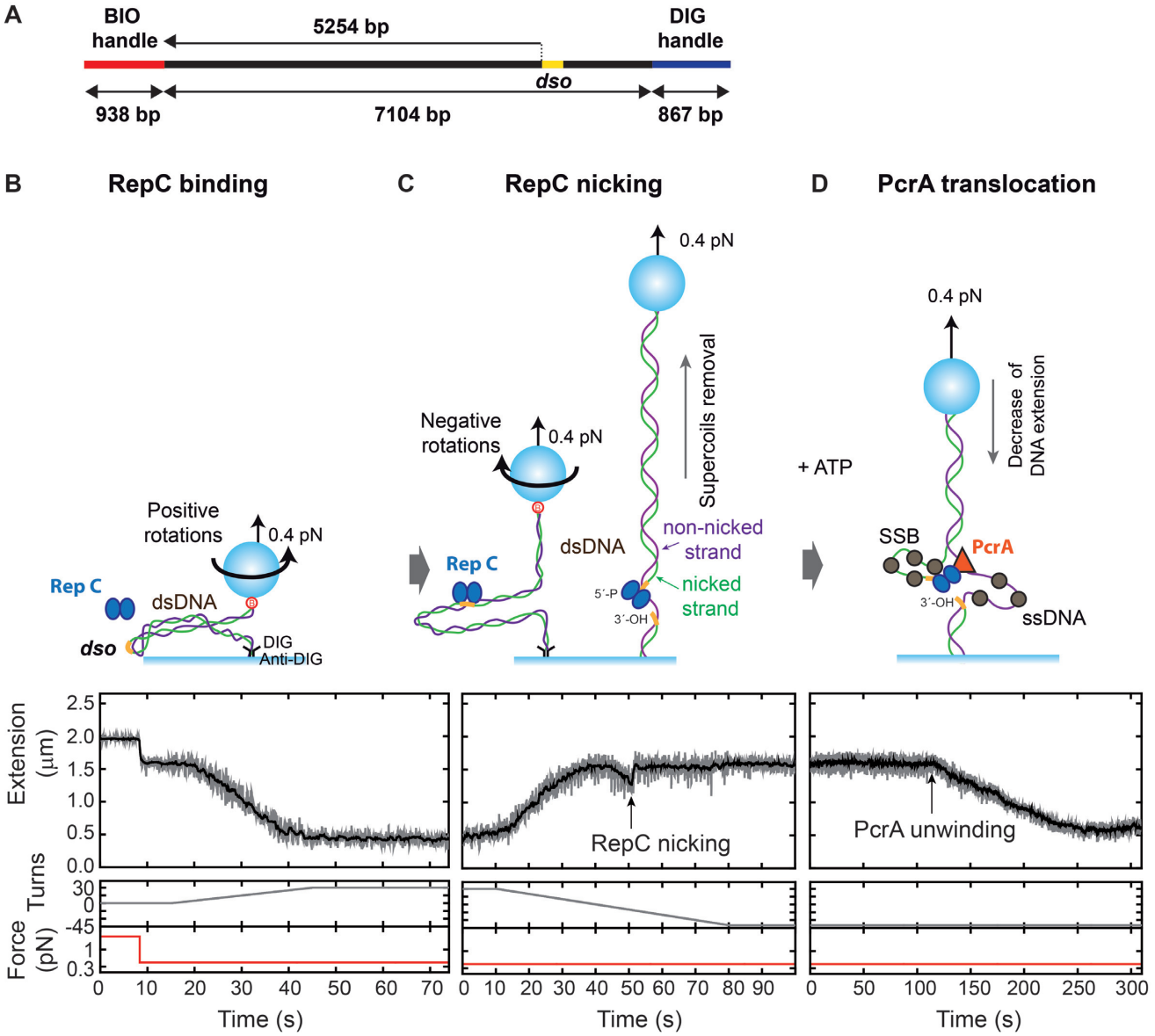

Figure 2. MT assay to investigate DNA nicking and unwinding by RepC and PcrA. (**A**) *Long-run* DNA substrate employed for the MT assay. It contains two handles labelled with biotins and digoxigenins and a central part with the *dso* at 5254 bp (nicking site at 5289 bp) from the biotinylated DNA end. (**B**) DNAs are first positively supercoiled and incubated with the RepC protein. (**C**) Magnet rotations are changed from positive to negative turns and RepC nicks the DNA; a sudden increase of extension due to the removal of supercoils is observed. Note that the DNA molecule remains nicked as it does not change the extension with rotations. (**D**) PcrA, SSB and ATP are added to the reaction. DNA unwinding by PcrA results in a reduction of the extension. SSB protein binds to the resulting ssDNA. Lower graphs represent the applied force (red) and magnet turns (grey) versus time. Raw data were acquired at 60 Hz and filtered down to 3 Hz.

potential effect that the production of ssDNA might have on the helicase activity. PcrA processivity was measured as single translocation events including pauses and was, within error, constant with PcrA concentration with a mean value of 3766 ± 76 bp (mean ± standard error of the mean (SEM)) (Figure 3A, black bars; Supplementary Table S2). This likely reflects the activity of individual PcrA molecules and confirms the high processivity of the enzyme in the presence of Rep protein, as reported previously (16). We used *E. coli* SSB to prevent formation of secondary structures on the ssDNA produced by the helicase. The presence of SSB slightly increased PcrA processivity to a mean value of 4533 ± 145 bp (mean ± SEM) compared to experiments performed in the absence of SSB (Figure 3A). Moreover, the presence of SSB protein prevented rehybridization events as occasionally found with naked DNA, likely because SSB coats the nascent ssDNA produced by the helicase. This significantly increased the difference of processivity when considering extensions at equilibrium, i.e. after any partial rehybridization event (Supplementary Figure S9). Taken together, our data support an enhanced PcrA processivity in the presence of the SSB protein likely by preventing partial reannealing events (see later; Supplementary Figure S9). Processivity data with the alternative *short-run* DNA construct did not show, within the margin of error, any difference between experiments with and with-

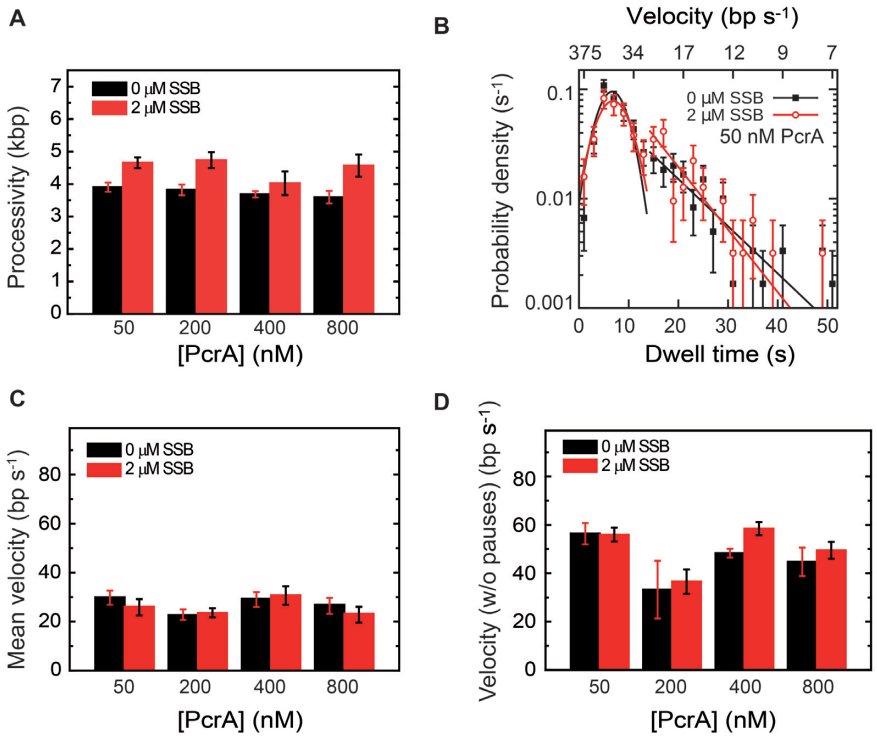

Figure 3. PcrA processivity and unwinding rates. (**A**) Mean values of DNA unwinding length or PcrA processivity. (**B**) Dwell time distributions for PcrA (50 mM) unwinding windows of 375 bp in the absence and in the presence of 2 μM SSB (black solid squares and red open circles, respectively). Solid lines are (i) fits to a Gaussian function for times shorter than 13 s revealing a characteristic velocity distribution in the absence of pauses and (ii) exponential fits for times longer than 13 s, which are associated with pauses of stochastic nature. (**C**) Mean PcrA unwinding rates including pausing. (**D**) Pause-free unwinding rates. All the experiments were performed at a constant monomeric RepC concentration of 200 nM and at varied PcrA concentrations (50, 200, 400 and 800 nM). Data obtained in the absence of SSB (black bars) and in the presence of 2 μM SSB proteins (red bars). Error bars in (A) are SEM. Error bars in (C) represent the 95% confidence intervals obtained from bootstrapping the data 10 000 times. Error bars in (D) represent the error of the Gaussian fit to the dwell time distribution. See Supplementary Tables S2 and S3 for a summary of conditions and mean dynamic parameters.

out the SSB protein (Supplementary Figure S10A). This was expected because the length available for unwinding in the *short-run* DNA is much shorter than for the *long-run* DNA.

Unwinding rates and pausing were characterized following previously published methods based on the analysis of dwell times for translocating a fixed distance (35). Details of the procedure can be found in 'Materials and Methods' section and Supplementary Methods. We obtained probability distributions of dwell times, from where we extracted mean translocation rates with/without pauses and pause rates (Figure 3B, Supplementary Figure S3). Mean translocation rates considering pausing (Equation (S6)) were found to be independent of helicase concentration with a mean value of 27 ± 3 bp s^{-1} (Figure 3C). In the presence of the SSB protein, we obtained a mean translocation rate of 26 ± 3 bp s^{-1} (Figure 3C). In addition, our dwell time analysis allowed us to determine a characteristic pause-free velocity of PcrA of 46 ± 6 bp s^{-1} (Figure 3D, Supplementary Table S2, Equations (S7) and (S8)). The presence of the SSB protein did not affect the pause-free velocity of PcrA. Complementary experiments using the *short-run* DNA construct at 200 nM RepC and 50 nM PcrA provided uniform and essentially pause-free unwinding traces with a mean unwinding rate of 50 bp s^{-1} in the presence and absence of SSB (Supplementary Figure S10B).

Dwell time distributions also showed a decaying tail that is attributed to stochastic PcrA pausing. From these data, we obtained an estimation of the rate to exit the pause state, $k_{off} = 0.112 \pm 0.004$ s^{-1} (Supplementary Figure S3C, Supplementary Table S2). The total number of pauses gave an estimation of the pause entry rate, $k_{in} = 0.044 \pm 0.005$ s^{-1} (Supplementary Figure S3D, Supplementary Table S2). On average, PcrA paused every 680 bp with a lifetime of pause of 8.9 s. In the presence of SSB, unwinding events again exhibited short and stochastic pauses, which followed an exponential distribution (Supplementary Figure S3B) with a mean exit rate of $k_{off} = 0.108 \pm 0.005$ s^{-1} (Supplementary Figure S3C, Supplementary Table S3) and a frequency of pausing of $k_{in} = 0.041 \pm 0.005$ s^{-1} (Supplementary Figure S3D, Supplementary Table S3). Our detailed analysis of the mean translocation velocity, pause-free velocity and pause rates shows very similar values to those reported in the absence of SSB (Figure 3C and D; Supplementary Tables S2 and S3).

RepC and PcrA interaction prior to DNA nicking and unwinding

To study the potential interaction between RepC and PcrA during the nicking reaction, both proteins were incubated with positively supercoiled DNA in the presence of ATP. A

change from positive to negative rotations first triggered the nicking of the substrate by RepC and then PcrA translocation with a delay time of Δt between both events (Figure 4A). We analysed Δt and the number of turns required for RepC nicking, i.e. the linking number of the DNA at the nicking (ΔLk), for four different concentrations of PcrA up to 800 nM. The concentration of RepC monomer was maintained constant at 200 nM.

We found that PcrA concentration has a strong effect on Δt, showing shorter delays as the concentration of protein (or [PcrA]:[RepC] ratios) increases (Figure 4B). At high [PcrA]:[RepC] ratios, we observed multiple translocations that started within a time threshold of $\Delta t \leq 1.7$ s (Figure 4C). This time threshold is the minimum time required in our system to observe a translocation event occurring immediately after nicking and was determined by considering the translocation velocity of PcrA and fluctuations of the bead at 0.4 pN and 3 Hz bandwidth (∼18 nm). Indeed, we were unable to assign delay times below 1.7 s in ∼44% of the translocation time traces at PcrA concentrations over 400 nM (Figure 4C, Supplementary Table S2), suggesting that RepC might nick the DNA as a complex with PcrA (see later). However, at lower [PcrA]:[RepC] ratios, we systematically found larger delays, confirming that RepC nicking does not require the presence of PcrA, and indicating that the helicase can also bind to RepC after the nicking event and then unwind the DNA duplex, in agreement with a previous study (16).

The linking number required for RepC nicking, ΔLk, was also analysed for all PcrA concentrations. In the absence of PcrA, but using the translocation buffer supplemented with ATP, we obtained a mean $\Delta Lk = -9.3 \pm 0.5$ (mean ± SEM), similar to that reported previously (24). However, as the [PcrA]:[RepC] ratio increased, we noticed a shift to more negative values of ΔLk, up to -12.2 ± 0.3 at 800 nM PcrA concentration (Figure 4D, Supplementary Table S2). It may be argued that the extrusion of the cruciform needed for nicking would be dependent only on the torque and not by the supercoils *per se*. The torque being roughly constant after the buckling transition in tcDNA (38), ΔLk would be determined by the kinetics of the reaction (39). In our previous work, we showed that ΔLk was independent of the kinetics of the reaction by performing experiments at different magnet rotation rates (24). We here performed a similar experiment with 200 nM RepC and 400 nM PcrA (Supplementary Figure S11), and again, the frequency of magnet rotation did not affect ΔLk. Importantly, shorter delays Δt, obtained at high [PcrA]:[RepC] ratios, positively correlated with higher linking numbers ΔLk. This supports the idea of the formation of a RepC–PcrA complex prior to nicking that interacts with the DNA affecting the twist required for RepC nicking (Figure 4E). To further test this idea, we performed experiments where the fluid chamber was rinsed with several cell volumes of buffer after incubation of RepC and PcrA with positively supercoiled DNA. Then, we applied negative rotations to the DNA, observing nicking and unwinding activities, indicating that the complex can assemble on the DNA before RepC nicking (Supplementary Figure S12). Experiments using 2 μM SSB reproduced the same trend in Δt and ΔLk values observed in the absence of SSB. Similarly, delays between nicking and translocation were not affected by the presence of SSB (Figure 4F, Supplementary Tables S2 and S3).

Additional experiments were performed at a lower RepC concentration of 50 nM and different PcrA:RepC ratios (Supplementary Figure S13). At 1:1 ratio, we found $\Delta Lk = -8.8 \pm 0.3$ and mean delay $\Delta t = 20 \pm 8$ s ($N = 26$), consistent with the recruitment of PcrA after nicking. At 4:1 [PcrA]:[RepC] ratio, we again observed a shift in the linking number towards negative values $\Delta Lk = -11.8 \pm 0.4$ and a shorter mean delay $\Delta t = 8 \pm 2$ s ($N = 55$). These values were consistent with those obtained at similar protein ratios but using 200 nM RepC (Figure 4C and D, Supplementary Table S2). These experiments confirm that the negative shift observed in the linking number needed for nicking is not induced by the protein concentrations used, but likely reflects the interaction of the RepC–PcrA complex with the DNA structure prior to nicking.

Interaction of RepC and the RepC–PcrA complex with the DNA

With the aim to determine any potential twist on the DNA due to protein binding, we compared rotation–extension curves at 0.4 pN on naked DNA and after incubation with PcrA and/or a nicking-deficient RepC mutant ($RepC^{Y191S}$, which can bind to the DNA but cannot nick it; Supplementary Figure S1B). Rotation curves were fit to a parabolic function to determine the number of turns at maximum extension, i.e. where DNA is torsionally relaxed (Figure 5A). These parameters were compared with those obtained on the same DNA molecules prior to injection of protein, i.e. naked DNA, and in the presence of proteins (40). Experiments at 200 nM $RepC^{Y191S}$, 400 nM PcrA and 5 mM ATP (Figure 5B, green data) showed a mean negative shift in the position of the apex of the rotation curve of $\Delta R = -1.5 \pm 0.2$ turns (mean ± SEM), and a reduction of the extension of $\Delta Z = -44 \pm 17$ nm (mean ± SEM, $N = 35$). To determine whether this extra untwist was induced by RepC or PcrA, we repeated the same experiment in the absence of PcrA (Figure 5B, red data). We obtained very similar values for the rotation shift and the change in extension ($\Delta R = -1.3 \pm 0.2$ turns and $\Delta z = -36 \pm 13$ nm, respectively, $N = 43$), suggesting that the extra untwist was induced only by RepC binding. A similar result was also obtained by using wild-type RepC in a buffer without Mg^{2+} to avoid nicking (data not shown). Control experiments in the presence of only PcrA (Figure 5B, purple data, $N = 22$), after injection of protein-free buffer (Figure 5B, black data, $N = 21$), and in the presence of just ATP (Figure 5B, blue data, $N = 35$) did not show any significant shift in rotation and extension.

The values of rotation shift ΔR were also measured in the regular nicking–unwinding MT assay using wild-type RepC and PcrA proteins and a buffer containing Mg^{2+} and ATP. In these experiments, we compared the data with rotation curves of DNA obtained in the absence of proteins. An illustrative example is included in Figure 5C where a shift of ∼−1.5 turns with respect to naked DNA was detected in the presence of RepC or RepC and PcrA. Importantly,

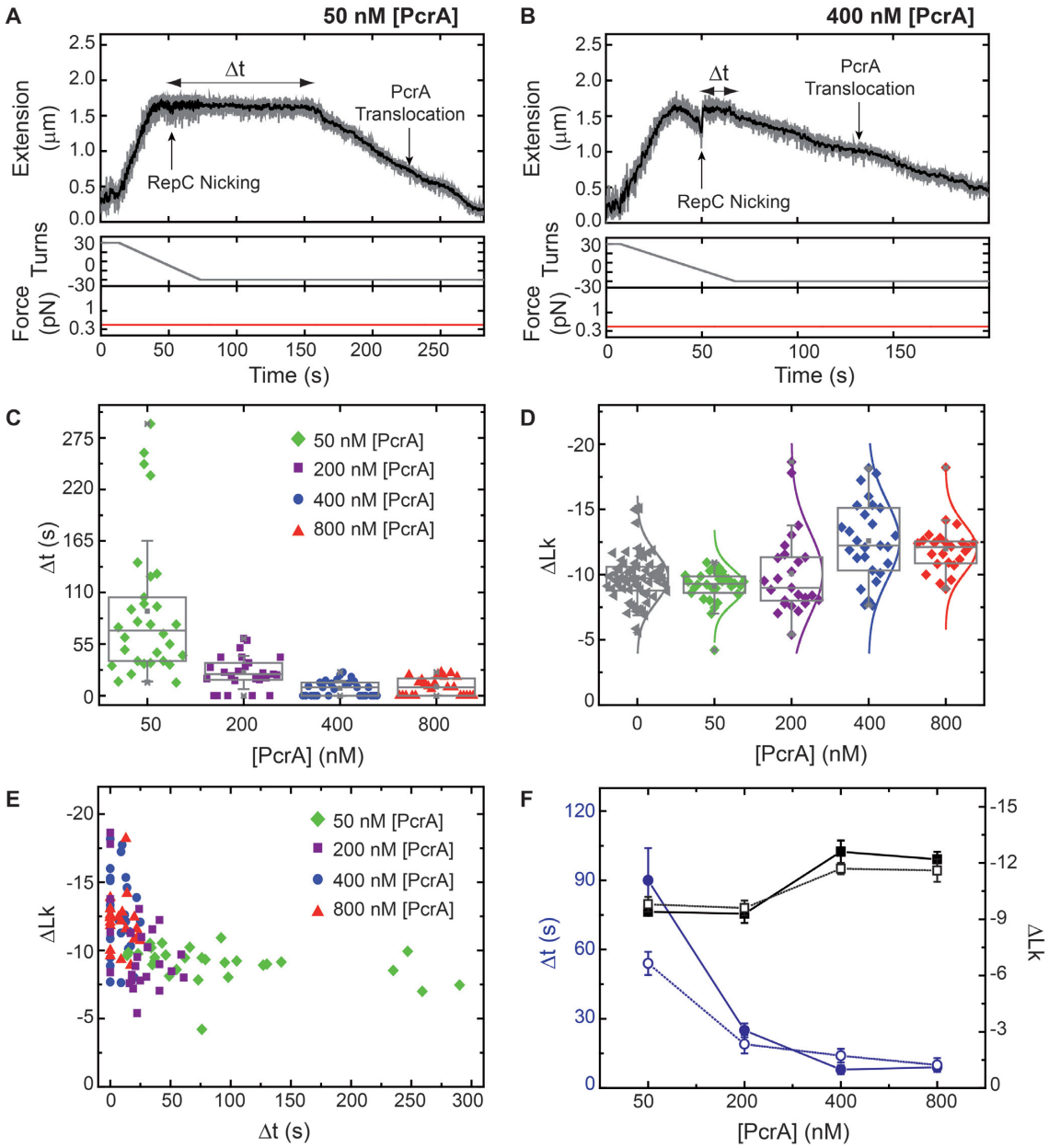

Figure 4. RepC–PcrA interaction during DNA nicking and unwinding. (**A**) Representative nicking–unwinding experiment performed at a low [PcrA]:[RepC] ratio (50 nM:200 nM). Typical delay times Δt of tens of seconds are obtained. (**B**) Representative nicking–unwinding experiment performed at high [PcrA]:[RepC] ratio (400 nM:200 nM). Delay times of a few seconds are obtained. (**C**) Delay times at different PcrA concentrations. (**D**) Shift in linking number required for nicking, ΔLk, at different PcrA concentrations. Box plots indicate the median, 25th and 75th percentiles of the distributions and the whiskers show the standard deviation. (**E**) Correlation between ΔLk and Δt for different PcrA concentrations. (**F**) Average supercoiling degree ΔLk and delay times Δt for different PcrA concentrations in the absence of SSB (solid symbols) or in the presence of 2 μM SSB (open symbols). RepC concentration was 200 nM for all experiments, magnets were rotated at 1 Hz and the applied force was 0.4 pN. See Supplementary Table S2 for a summary of conditions and mean dynamic parameters.

inclusion of PcrA in the reaction added ∼2 extra negative turns to the linking number ΔLk required for nicking (Figure 5D). This confirmed that the observed change in twist with RepC^{Y191S} was not a consequence of the mutation of the nicking residue.

Taken together, our data indicate that RepC binding induces untwisting on the DNA by -1.5 ± 0.2 turns. The experiment including the nicking mutant and PcrA did not add additional untwist. We propose that the three extra negative turns needed to nick the DNA arise from the structure of the RepC–PcrA protein complex, which requires some extra negative turns to position the DNA nicking site at the catalytic site of RepC (see 'Discussion' section).

DISCUSSION

A key step in the RCR is the unwinding of dsDNA by the PcrA helicase, a step critically dependent upon the genera-

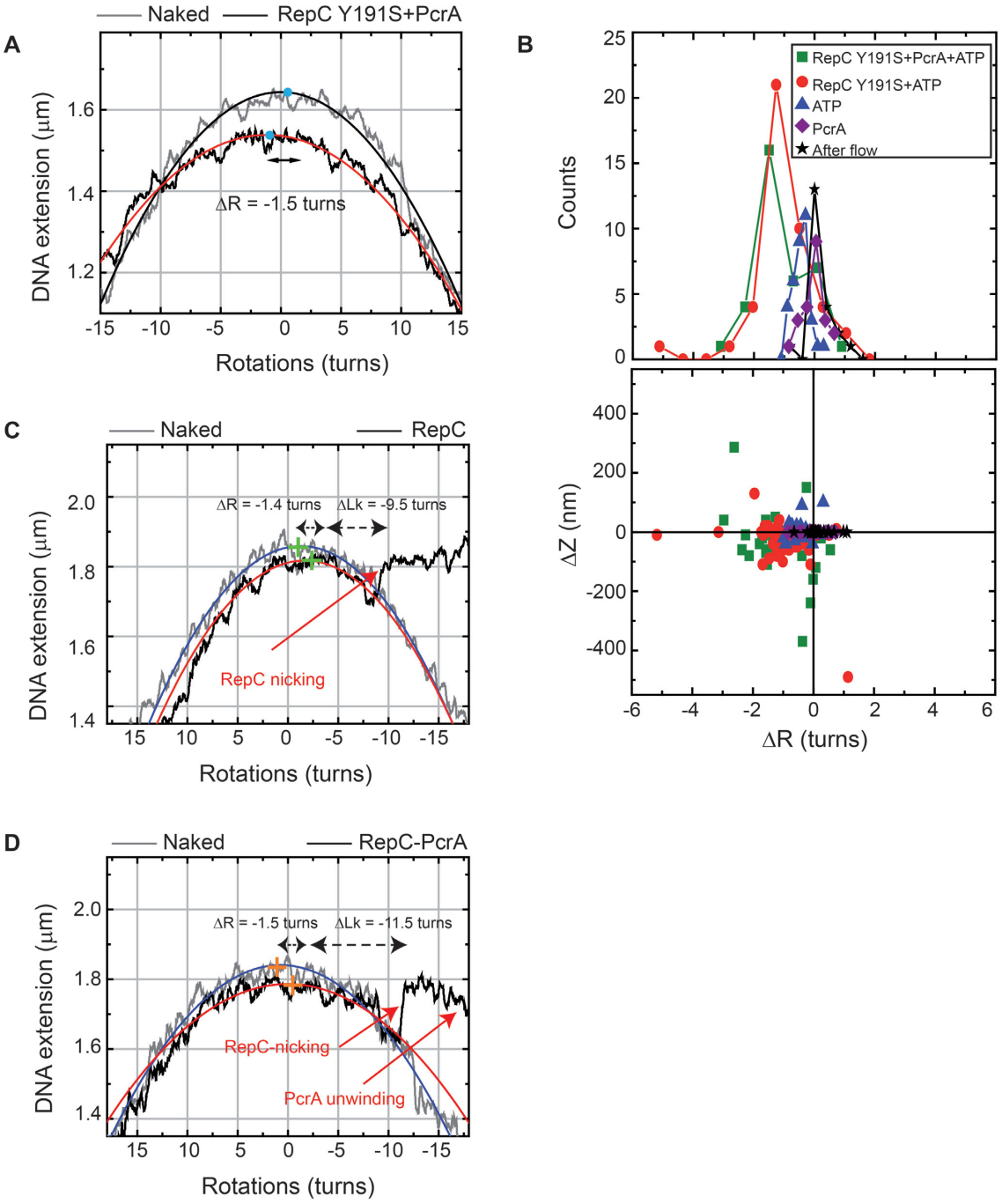

Figure 5. RepC binding induces untwisting of DNA. (**A**) Rotation–extension curves in the absence (grey) and presence of RepC^{Y191S} mutant and PcrA proteins (black). A fit of a parabola within the range of −15 to +15 rotations is included to illustrate the procedure to determine R_{max} and Z_{max} (see 'Materials and Methods' section). In this particular example, we observed a shift of $\Delta R = -1.5$ turns and $\Delta Z = -100$ nm. (**B**) Shifts of extensions and rotations (ΔZ, ΔR) under different experimental conditions: RepC^{Y191S}, PcrA and ATP (green squares, $N = 35$); RepC^{Y191S} and ATP (red circles, $N = 43$); ATP (blue triangles, $N = 35$); PcrA (purple diamonds, $N = 22$) and buffer (black stars, $N = 21$). RepC^{Y191S} and PcrA concentrations were 200 and 800 nM, respectively. Data in the upper panel are binned. Data in the lower panel represent individual molecules. Experiments showing the shifts produced by RepC binding and nicking in the absence (**C**) and presence (**D**) of PcrA. RepC and PcrA concentrations were 200 and 400 nM, respectively, for these experiments.

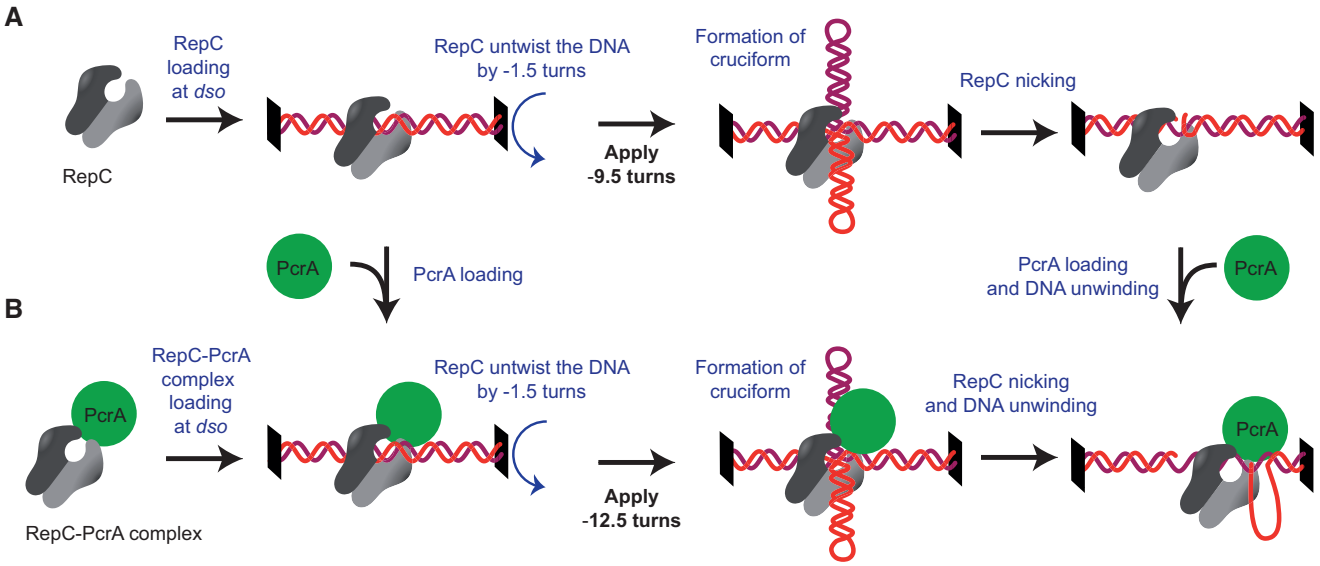

Figure 6. Model of RepC–PcrA complex interaction with the DNA. (**A**) PcrA is recruited after RepC nicking (low [PcrA]:[RepC] ratio). The binding of RepC to DNA induces the unwinding of −1.5 turns of the DNA. Then, RepC requires −9.5 additional turns for cruciform extrusion and nicking. After the nicking reaction, PcrA is recruited by RepC and unwinds the duplex in complex with RepC. (**B**) RepC–PcrA complex assembles on the DNA before RepC nicking (high [PcrA]:[RepC] ratio). The binding of RepC induces DNA unwinding by −1.5 turns, as in the absence of PcrA. However, in complex with PcrA, RepC requires −12.5 turns for nicking, ∼3 extra turns compared to pathway (A).

tion of a nick by the replication initiator protein, Rep. Here, we have developed an MT assay to investigate the interplay between both proteins and their interactions with the DNA as isolated components and as a complex. Our assay allows us to monitor both the nicking and unwinding reactions and to correlate protein activity with changes in the topology of DNA. This information is not accessible to single-molecule fluorescent imaging or to bulk biochemical measurements. We have discovered that RepC and PcrA can form a complex on the DNA prior to the nicking reaction (Supplementary Figure S12). Our results indicate that once the complex is formed, extra negative twisting of DNA is required to initiate nicking, which is followed by the unwinding of the DNA by the helicase.

Our single-molecule experiments indicate that PcrA is capable of unwinding thousands of base pairs resulting in full unwinding of plasmid-size DNA substrates (∼5 kb). We found a mean unwinding rate of ∼30 bp s^{-1} (Figure 3C) dominated by short pauses of stochastic nature. This is roughly in agreement with data reported for *Bs*PcrA in stopped-flow fluorescence assays using a fluorescently labelled SSB protein (19,41) and in single-molecule total internal reflection fluorescence (TIRF) assays, both using kb long dsDNA substrates (16). The pausing of PcrA might be attributed to backtracking and/or to the interaction with particular DNA sequences. In our case, the large window employed for the dwell time analysis (conditioned by the fluctuations in extension at low force) does not allow us to attribute pauses to specific DNA sequences. We speculate that frequent PcrA pausing facilitates the eventual recognition of the *dso* by RepC, a requirement for the termination of the RCR. Our thorough dwell time analysis revealed a peak of unwinding rate of ∼50 bp s^{-1} (Figure 3D). This result is consistent with the translocation velocity of *Bs*PcrA reported in experiments using short oligo ssDNA substrates (18–80 bases), where the probability of pausing is negligible (17,42). In our experiments, the presence of the SSB protein did not affect the unwinding rate of PcrA (Figure 3C), but prevented ssDNA rehybridization (Supplementary Figure S7), resulting in an increase in the processivity of PcrA (Figure 3A and B). This has been previously reported for DNA repair helicases, RecA nucleoprotein formation and in the RCR process itself (43–47).

We next investigated the interaction of RepC and PcrA and the potential influence of the helicase on RepC nicking. Previous evidence of interaction between RepC and PcrA from different organisms comes from pull-down assays (8,14,48) and from experiments that required PcrA for DNA unwinding of plasmids (18). Also, evidence of interaction between RepD and PcrA has been reported from reactions that contained substrate DNA pre-nicked by RepD (7,16,18); these assays could not reveal whether both proteins already in a complex could nick the DNA. Experiments at low [PcrA]:[RepC] ratios reported a delay time between nicking and unwinding consistent with the recruitment of PcrA by RepC at the *dso* after nicking. However, at high [PcrA]:[RepC] ratios we observed multiple events of PcrA translocation (42%), concomitant within our time resolution, with RepC nicking (Figure 4C, Supplementary Table S2). The same observation was obtained at a lower RepC concentration (50 nM) and equivalent [PcrA]:[RepC] ratios (Supplementary Figure S13). These data support the idea that a stable complex between RepC and PcrA can be formed before RepC nicking. This idea is further supported by the correlation between delay times and the shift in the number of negative supercoils required for nicking (Figure 4E) and the experiment where the fluid chamber was rinsed with several cell volumes after protein incubation (Supplementary Figure S12). Nonetheless, we cannot rule out the recruitment of PcrA at the *dso*, after RepC nicking, at rates

faster than the resolution of our instrument to detect DNA unwinding (1.7 s). This would explain cases where we do not observe the shift in ΔLk but measure straight unwinding after nicking. Regardless, the dependence of the correlation between Δt and ΔLk with the [PcrA]:[RepC] ratio rules out a model where the rate-limiting step for the initiation of unwinding is the reorganization of the RepC–PcrA complex to adopt an active conformation (7).

At high [PcrA]:[RepC] ratios, we found that the RepC nicking activity is significantly influenced by its interaction with PcrA. On average, three additional negative turns were required to trigger RepC nicking when complexed with PcrA. Experiments in the presence of the SSB protein did not alter this result. A possible explanation for the increase in the number of turns observed here is that PcrA is directly affecting the kinetics of the reaction. However, this possibility was ruled out because the frequency of magnet rotation did not affect ΔLk (Supplementary Figure S11). An alternative explanation for the additional turns observed for nicking is that the conformational space of the cruciform suitable for RepC nicking is constrained in the presence of PcrA. This idea is consistent with the model proposed by Carr et al. for Rep–DNA binding and PcrA recruitment (49). These authors solved the structure of *S. aureus* RepDE heterodimer, revealing a C-shaped configuration, with the catalytic tyrosines and DNA binding residues inside and outside the cavity, respectively. In their model, PcrA is bound in front of the Rep dimer, resulting in an O-shaped structure that embraces the extruded DNA cruciform in a precise configuration. Based on these ideas, we have previously constructed a model where negative turns are needed to extrude a cruciform structure to place the DNA nicking site in the vicinity of the RepC active site (24). We propose that the binding of PcrA to RepC triggers a conformational change in RepC. This would restrict the conformational space of the cruciform suitable for RepC nicking and, as a consequence, select for those cruciform conformations with a larger energy extrusion barrier, i.e. requiring additional negative turns to be produced.

The shift in number of turns for RepC nicking in the presence of PcrA led us to study the topological implications of RepC and PcrA binding on the DNA by using a RepC variant that can bind but not nick the DNA. Interestingly, we found that the protein untwists the DNA by ~ -1.5 turns on average; i.e. it unwinds $\sim$16 bp of DNA. We have previously reported that RepC nicking is passive because the energy to extrude the cruciform is mostly extracted from the natural supercoiling of the plasmid, rather than from a twist induced by the protein. Our conclusions were based on the typical free energy barrier for cruciform extrusion ($\sim$40 kcal mol^{-1}) (50) and by the supercoiling energies determined from the experiments. In this work, we have found that RepC binding induces a variation of twist of ~ -1.5 turns in the DNA. One could argue that this twist might be sufficient to extrude the cruciform structure. We show later that the elastic energy stored in 1.5 turns is not enough to supercoil the DNA. The elastic energy of a twisted isotropic rod is given by $E = 2\pi^2 C k_B T L^{-1} \Delta R^2$, where L and C are the contour length and torsional modulus of the DNA, respectively, and ΔR is the shift in turns (51). At the force employed in this work, and considering $C \sim 65$ nm (52), we obtain an elastic energy of $E \sim 0.7$ kcal mol^{-1}. This energy is slightly above the average thermal energy of the environment, thus reflecting a minimal contribution of RepC on cruciform extrusion and favouring the passive model described in our previous work.

In cells, the RepC nicking activity triggered in our experiments by supercoiling the DNA with the magnets would be prompted by the natural supercoiling degree of the DNA as a result of the action of topoisomerases. We have previously argued that the supercoiling degree required for nicking was similar to that found *in vivo* (24). The change in the number of turns necessary for RepC nicking in the presence of PcrA is still small compared with the total number of turns necessary for RepC nicking alone. Thus, we can consider that, while the presence of PcrA increases the energy barrier for nicking, this change is small compared to that necessary for RepC nicking alone. We speculate that the supercoiling dependence of RepC nicking activity is probably a mechanism for the replication of the plasmid, such that the process is only possible once a certain degree of compaction through plectoneme formation is reached.

We have combined our new findings on the interplay between RepC and PcrA for DNA nicking and unwinding in an updated model for RepC nicking that includes the effect of its interaction with PcrA (Figure 6). We found that RepC untwists the DNA by ~ -1.5 turns. However, this is not enough to extrude the cruciform needed for DNA nicking. In the absence of PcrA, DNA must be still untwisted by ~ -9.5 turns, as we previously reported (24). PcrA can be later loaded at the RepC–DNA site and unwind the DNA (Figure 6A). However, in the presence of PcrA, both proteins can form a complex at the binding site and this implies -3 additional unwinding turns to observe nicking on the DNA (Figure 6B). In this scenario, DNA unwinding starts immediately because the helicase is already present at the nicking site. Our MT methodology has allowed us to recapitulate the initial two steps of the RCR mechanism by coupling RepC, PcrA and SSB activities in a single-molecule assay. Our work provides a basis to investigate the DNA synthesis and termination steps of RCR, with a final aim to recapitulate the whole process of RCR at the single-molecule level.

SUPPLEMENTARY DATA

Supplementary Data are available at NAR Online.

ACKNOWLEDGEMENTS

The authors are grateful to Prof. Mark S. Dillingham and his group for critical discussion of this work. The authors are also grateful to all members of the Moreno-Herrero lab for discussion of data and fruitful discussions.
Authors' contributions: C.C. and C.L.P. performed research and analysed data. C.C., C.L.P. and F.M.-H. designed research. C.A.-R. produced DNA constructs and proteins. S.H.L. and S.A.K. provided protein expression constructs and produced proteins. F.M.-H. wrote the original draft of the paper. All authors contributed to discussion of data, review and editing of the manuscript.

FUNDING

Ministerio de Economía y Competitividad (MINECO) [BFU2017-83794-P (AEI/FEDER, UE) to F.M.-H.]; European Research Council (ERC) under the European Union Horizon 2020 research and innovation grant agreement [681299 to F.M.-H.]; National Science Foundation [to S.H.L.]. C.C. was supported by a 'Severo Ochoa' postdoctoral contract from the National Center of Biotechnology (CNB-CSIC); Funding for open access charge: European Research Council [681299].

Conflict of interest statement. None declared.

REFERENCES

1. Kornberg,R.D. and Lorch,Y. (1992) Chromatin structure and transcription. *Annu. Rev. Cell Biol.*, **8**, 563–587.
2. Khan,S.A. (1997) Rolling-circle replication of bacterial plasmids. *Microbiol. Mol. Biol. Rev.*, **61**, 442–455.
3. Ruiz-Maso,J.A., Macho,N.C., Bordanaba-Ruiseco,L., Espinosa,M., Coll,M. and Del Solar,G. (2015) Plasmid rolling-circle replication. *Microbiol.Spectr.*, **3**, doi:10.1128/microbiolspec.PLAS-0035-2014.
4. Silver,S. (1996) Bacterial resistances to toxic metal ions—a review. *Gene*, **179**, 9–19.
5. Gordon,J.E. and Christie,P.J. (2014) The *Agrobacterium* Ti plasmids. *Microbiol. Spectr.*, **2**, doi:10.1128/microbiolspec.PLAS-0010-2013.
6. Thomas,C.D., Balson,D.F. and Shaw,W.V. (1990) *In vitro* studies of the initiation of staphylococcal plasmid replication. Specificity of RepD for its origin (oriD) and characterization of the Rep-ori tyrosyl ester intermediate. *J. Biol. Chem.*, **265**, 5519–5530.
7. Machon,C., Lynch,G.P., Thomson,N.H., Scott,D.J., Thomas,C.D. and Soultanas,P. (2010) RepD-mediated recruitment of PcrA helicase at the *Staphylococcus aureus* pC221 plasmid replication origin, oriD. *Nucleic Acids Res.*, **38**, 1874–1888.
8. Chang,T.L., Naqvi,A., Anand,S.P., Kramer,M.G., Munshi,R. and Khan,S.A. (2002) Biochemical characterization of the *Staphylococcus aureus* PcrA helicase and its role in plasmid rolling circle replication. *J. Biol. Chem.*, **277**, 45880–45886.
9. Zhang,W., Dillingham,M.S., Thomas,C.D., Allen,S., Roberts,C.J. and Soultanas,P. (2007) Directional loading and stimulation of PcrA helicase by the replication initiator protein RepD. *J. Mol. Biol.*, **371**, 336–348.
10. Kramer,M.G., Khan,S.A. and Espinosa,M. (1997) Plasmid rolling circle replication: identification of the RNA polymerase-directed primer RNA and requirement for DNA polymerase I for lagging strand synthesis. *EMBO J.*, **16**, 5784–5795.
11. del Solar,G., Giraldo,R., Ruiz-Echevarria,M.J., Espinosa,M. and Diaz-Orejas,R. (1998) Replication and control of circular bacterial plasmids. *Microbiol. Mol. Biol. Rev.*, **62**, 434–464.
12. Petit,M.A., Dervyn,E., Rose,M., Entian,K.D., McGovern,S., Ehrlich,S.D. and Bruand,C. (1998) PcrA is an essential DNA helicase of *Bacillus subtilis* fulfilling functions both in repair and rolling-circle replication. *Mol. Microbiol.*, **29**, 261–273.
13. Iordanescu,S. (1993) Characterization of the *Staphylococcus aureus* chromosomal gene *pcrA*, identified by mutations affecting plasmid pT181 replication. *Mol. Gen. Genet.*, **241**, 185–192.
14. Anand,S.P., Mitra,P., Naqvi,A. and Khan,S.A. (2004) *Bacillus anthracis* and *Bacillus cereus* PcrA helicases can support DNA unwinding and *in vitro* rolling-circle replication of plasmid pT181 of *Staphylococcus aureus*. *J. Bacteriol.*, **186**, 2195–2199.
15. Velankar,S.S., Soultanas,P., Dillingham,M.S., Subramanya,H.S. and Wigley,D.B. (1999) Crystal structures of complexes of PcrA DNA helicase with a DNA substrate indicate an inchworm mechanism. *Cell*, **97**, 75–84.
16. Chisty,L.T., Toseland,C.P., Fili,N., Mashanov,G.I., Dillingham,M.S., Molloy,J.E. and Webb,M.R. (2013) Monomeric PcrA helicase processively unwinds plasmid lengths of DNA in the presence of the initiator protein RepD. *Nucleic Acids Res.*, **41**, 5010–5023.
17. Dillingham,M.S., Wigley,D.B. and Webb,M.R. (2000) Demonstration of unidirectional single-stranded DNA translocation by PcrA helicase: measurement of step size and translocation speed. *Biochemistry*, **39**, 205–212.
18. Soultanas,P., Dillingham,M.S., Papadopoulos,F., Phillips,S.E., Thomas,C.D. and Wigley,D.B. (1999) Plasmid replication initiator protein RepD increases the processivity of PcrA DNA helicase. *Nucleic Acids Res.*, **27**, 1421–1428.
19. Slatter,A.F., Thomas,C.D. and Webb,M.R. (2009) PcrA helicase tightly couples ATP hydrolysis to unwinding double-stranded DNA, modulated by the initiator protein for plasmid replication, RepD. *Biochemistry*, **48**, 6326–6334.
20. Koepsel,R.R., Murray,R.W., Rosenblum,W.D. and Khan,S.A. (1985) The replication initiator protein of plasmid pT181 has sequence-specific endonuclease and topoisomerase-like activities. *Proc. Natl. Acad. Sci. U.S.A.*, **82**, 6845–6849.
21. Koepsel,R.R., Murray,R.W. and Khan,S.A. (1986) Sequence-specific interaction between the replication initiator protein of plasmid pT181 and its origin of replication. *Proc. Natl. Acad. Sci. U.S.A.*, **83**, 5484–5488.
22. Dempsey,L.A., Birch,P. and Khan,S.A. (1992) Six amino acids determine the sequence-specific DNA binding and replication specificity of the initiator proteins of the pT181 family. *J. Biol. Chem.*, **267**, 24538–24543.
23. Zhao,A.C., Ansari,R.A., Schmidt,M.C. and Khan,S.A. (1998) An oligonucleotide inhibits oligomerization of a rolling circle initiator protein at the pT181 origin of replication. *J. Biol. Chem.*, **273**, 16082–16089.
24. Pastrana,C.L., Carrasco,C., Akhtar,P., Leuba,S.H., Khan,S.A. and Moreno-Herrero,F. (2016) Force and twist dependence of RepC nicking activity on torsionally-constrained DNA molecules. *Nucleic Acids Res.*, **44**, 8885–8896.
25. Toleikis,A., Webb,M.R. and Molloy,J.E. (2018) oriD structure controls RepD initiation during rolling-circle replication. *Sci. Rep.*, **8**, 1206.
26. Chang,T.L., Kramer,M.G., Ansari,R.A. and Khan,S.A. (2000) Role of individual monomers of a dimeric initiator protein in the initiation and termination of plasmid rolling circle replication. *J. Biol. Chem.*, **275**, 13529–13534.
27. Khan,S.A. and Novick,R.P. (1983) Complete nucleotide sequence of pT181, a tetracycline-resistance plasmid from *Staphylococcus aureus*. *Plasmid*, **10**, 251–259.
28. Fili,N., Mashanov,G.I., Toseland,C.P., Batters,C., Wallace,M.I., Yeeles,J.T., Dillingham,M.S., Webb,M.R. and Molloy,J.E. (2010) Visualizing helicases unwinding DNA at the single molecule level. *Nucleic Acids Res.*, **38**, 4448–4457.
29. Strick,T.R., Allemand,J.F., Bensimon,D. and Croquette,V. (1998) Behavior of supercoiled DNA. *Biophys. J.*, **74**, 2016–2028.
30. Seidel,R., van Noort,J., van der Scheer,C., Bloom,J.G., Dekker,N.H., Dutta,C.F., Blundell,A., Robinson,T., Firman,K. and Dekker,C. (2004) Real-time observation of DNA translocation by the type I restriction modification enzyme EcoR124I. *Nat. Struct. Mol. Biol.*, **11**, 838–843.
31. te Velthuis,A.J., Kerssemakers,J.W., Lipfert,J. and Dekker,N.H. (2010) Quantitative guidelines for force calibration through spectral analysis of magnetic tweezers data. *Biophys. J.*, **99**, 1292–1302.
32. Daldrop,P., Brutzer,H., Huhle,A., Kauert,D.J. and Seidel,R. (2015) Extending the range for force calibration in magnetic tweezers. *Biophys. J.*, **108**, 2550–2561.
33. Bosco,A., Camunas-Soler,J. and Ritort,F. (2014) Elastic properties and secondary structure formation of single-stranded DNA at monovalent and divalent salt conditions. *Nucleic Acids Res.*, **42**, 2064–2074.
34. Fuentes-Perez,M.E., Dillingham,M.S. and Moreno-Herrero,F. (2013) AFM volumetric methods for the characterization of proteins and nucleic acids. *Methods*, **60**, 113–121.
35. Dulin,D., Vilfan,I.D., Berghuis,B.A., Poranen,M.M., Depken,M. and Dekker,N.H. (2015) Backtracking behavior in viral RNA-dependent RNA polymerase provides the basis for a second initiation site. *Nucleic Acids Res.*, **43**, 10421–10429.
36. Efron,B. and Tibshirani,R.J. (1994) *An Introduction to the Bootstrap*. Chapman & Hall/CRC, London.
37. Smith,S.B., Cui,Y. and Bustamante,C. (1996) Overstretching B-DNA: the elastic response of individual double-stranded and single-stranded DNA molecules. *Science*, **271**, 795–799.
38. Mosconi,F., Allemand,J.F., Bensimon,D. and Croquette,V. (2009) Measurement of the torque on a single stretched and twisted DNA using magnetic tweezers. *Phys. Rev. Lett.*, **102**, 078301.

39. Rutkauskas,M., Krivoy,A., Szczelkun,M.D., Rouillon,C. and Seidel,R. (2017) Single-molecule insight into target recognition by CRISPR–Cas complexes. *Methods Enzymol.*, **582**, 239–273.
40. Zorman,S., Seitz,H., Sclavi,B. and Strick,T.R. (2012) Topological characterization of the DnaA–oriC complex using single-molecule nanomanipuation. *Nucleic Acids Res.*, **40**, 7375–7383.
41. Arbore,C., Lewis,L.M. and Webb,M.R. (2012) Kinetic mechanism of initiation by RepD as a part of asymmetric, rolling circle plasmid unwinding. *Biochemistry*, **51**, 3684–3693.
42. Park,J., Myong,S., Niedziela-Majka,A., Lee,K.S., Yu,J., Lohman,T.M. and Ha,T. (2010) PcrA helicase dismantles RecA filaments by reeling in DNA in uniform steps. *Cell*, **142**, 544–555.
43. Stano,N.M., Jeong,Y.J., Donmez,I., Tummalapalli,P., Levin,M.K. and Patel,S.S. (2005) DNA synthesis provides the driving force to accelerate DNA unwinding by a helicase. *Nature*, **435**, 370–373.
44. Rajagopal,V. and Patel,S.S. (2008) Single strand binding proteins increase the processivity of DNA unwinding by the hepatitis C virus helicase. *J. Mol. Biol.*, **376**, 69–79.
45. Yeeles,J.T., van Aelst,K., Dillingham,M.S. and Moreno-Herrero,F. (2011) Recombination hotspots and single-stranded DNA binding proteins couple DNA translocation to DNA unwinding by the AddAB helicase–nuclease. *Mol. Cell*, **42**, 806–816.
46. Roy,R., Kozlov,A.G., Lohman,T.M. and Ha,T. (2009) SSB protein diffusion on single-stranded DNA stimulates RecA filament formation. *Nature*, **461**, 1092–1097.
47. Ducani,C., Bernardinelli,G. and Hogberg,B. (2014) Rolling circle replication requires single-stranded DNA binding protein to avoid termination and production of double-stranded DNA. *Nucleic Acids Res.*, **42**, 10596–10604.
48. Ruiz-Maso,J.A., Anand,S.P., Espinosa,M., Khan,S.A. and del Solar,G. (2006) Genetic and biochemical characterization of the *Streptococcus pneumoniae* PcrA helicase and its role in plasmid rolling circle replication. *J. Bacteriol.*, **188**, 7416–7425.
49. Carr,S.B., Phillips,S.E. and Thomas,C.D. (2016) Structures of replication initiation proteins from staphylococcal antibiotic resistance plasmids reveal protein asymmetry and flexibility are necessary for replication. *Nucleic Acids Res.*, **44**, 2417–2428.
50. Lilley,D.M.J. (1989) Structural isomerization in DNA: the formation of cruciform structures in supercoiled DNA molecules. *Chem. Soc. Rev.*, **18**, 53–83.
51. Marko,J.F. (2007) Torque and dynamics of linking number relaxation in stretched supercoiled DNA. *Phys. Rev. E: Stat. Nonlin. Soft Matter Phys.*, **76**, 021926.
52. Lipfert,J., Wiggin,M., Kerssemakers,J.W., Pedaci,F. and Dekker,N.H. (2011) Freely orbiting magnetic tweezers to directly monitor changes in the twist of nucleic acids. *Nat. Commun.*, **2**, 439.